CONF-920144--2

ANL/CP--74004

DE92 006975

A FIRST LOOK AT EROSION OF CONTINUOUS-FIBER REINFORCED CERAMIC-MATRIX COMPOSITES*

K. R. Karasek, S. T. Gonczy
Allied-Signal Inc., Des Plaines, IL 60017

J. B. Kupperman, E. J. Zamirowski, K. C. Goretta, and J. L. Routbort†
Materials and Components Technology Division
†Materials Science Division
Argonne National Laboratory, Argonne, IL 60439

December 1991

DISCLAIMER

Manuscript to appear in American Ceramic Society Proceedings of the 16th Annual Conference on Composites and Advanced Ceramics, Cocoa Beach, FL, January 7-10, 1992.

*Work supported by the U.S. Department of Energy, BES-Materials Sciences, under contract #W-31-109-ENG-38 and by Allied-Signal Inc.

A FIRST LOOK AT EROSION OF CONTINUOUS-FIBER-REINFORCED CERAMIC-MATRIX COMPOSITES[¥]

K. R. Karasek*, S. T. Gonczy
Allied-Signal Inc., Des Plaines, IL 60017

J. B. Kupperman, E. J. Zamirowski, K. C. Goretta, J. L. Routbort
Argonne National Laboratory, Argonne, IL 60439

Abstract

We report the initial results of a study of solid-particle erosion of Nicalon™ SiC reinforced carbon-modified-silica-glass composites. SiC abrasives with diameters between 42 to 390μm were used with impact angles of 30° and 90°, and velocities ranged 30 to 80 m/s. Fibers were parallel to the surface in all cases. Woven-fiber composites exhibited the same erosive behavior as uniaxial composites. Interfacial chemistry was controlled, and the comparison between composites which exhibit low-strength-brittle and high-strength-fibrous fractures under flexure conditions showed no significant difference in erosion resistance. This result and SEM data indicate that most of the fracture occurs within the matrix and/or at the fiber-matrix interface. We have found in previous work that polymer-matrix composites (with fibers parallel to the surface) are more susceptible to erosion damage than the matrix polymer. This also appears to be the case for the ceramic composites.

Introduction

Fiber reinforced ceramic matrix composites offer the potential of dramatically improved toughness and fibrous failure. That translates into greater reliability and strength, as compared to monolithic ceramics. A fiber interface coating is required to produce the fibrous fracture; the stability of the interface determines the temperature stability of the system. With the development of interfaces with higher temperature capability, these composites will find an increasing number of applications out to 1000 °C.

The use of polymeric precursors to form the ceramic matrix offers significant fabrication advantages for ceramic composites of large and/or complex shapes. Allied-Signal's Blackglas™ ceramic (a carbon modified silica glass) is based on such a polymer precursor. Major airframe, engine, and component manufacturers are evaluating Blackglas™ composites for firewall, exhaust component, hot gas ducting, and dielectric applications.

Some potential applications involve erosive conditions. Glasses

¥ Work supported by the U.S. Dept. of Energy, BES-Materials Sciences under contract W-31-109-ENG-38 and by Allied-Signal Inc.

and ceramics are often considered to be fairly erosion-resistant compared to metals and polymers. Thus, it is tempting to assume that glass or ceramic composites will have similar properties -- particularly since the inclusion of fibers enhances the toughness and strength. However, this is not necessarily true. For example, in previous work we found that the introduction of high-strength carbon fibers to an epoxy matrix caused erosion resistance to decrease[1]. The purpose of this study, therefore, was to assess the erosion properties for Blackglas™ composites.

Experimental Procedure

A. Composite Fabrication

Five sets of materials were tested. Blackglas™ matrix composites were fabricated using Nicalon™ SiC fibers; these fibers have a pyrolytic carbon coating. A 31-cm-square composite plate (ASRT sample number 6222-26B) was made with 12 unidirectional tape plies (made by the drum-winding technique) in a 0/90 lay-up. Similarly a 20-cm-square composite panel (ASRT sample numbers 6325-3 & 3A) was fabricated using 10 plies of woven tape (8HS, 1800 denier). Each of these panels was cut in half, and one of the halves from each panel was then oxidized at 800 °C for 12 hours. The non-oxidized samples would exhibit fibrous (tough) fracture with flexure strength of approximately 350 MPa (50 ksi). The oxidation step removes the carbon surface layer and oxidizes the Nicalon™ fiber, filling the gap with SiO_2. Oxidized composites exhibit brittle failure and low strength (approximately 70 MPa [10 ksi]). Since a crack-free Blackglas™ monolith is extremely difficult to fabricate, commercially-available fused SiO_2 was used for control samples.

B. Erosion Measurements

A slinger-type apparatus described by Kosel, et al[2] was used. It consists of a vaccuum chamber resembling a flat drum that has sample holders positioned around its circumference. Erodent particles were accelerated by means of a rotating barrel. The velocity of the particles was fixed by the angular velocity of the rotating arm. The angle at which a sample was mounted determined the angle of attack of the particles. Angular spread depended upon the absolute angle; it is 3° at 30° and 7° at 90°. Vacuum was maintained between 67 kPa and 100 kPa in order to eliminate air resistance on the rotating barrel.

For the composites made with uniaxial plies, the surface ply did have a specific orientation. To test for the effect of orientation, the panels were tested in horizontal and vertical modes. The difference between these orientations can be seen by considering the projection of the line traced by the path of an eroding particle onto the plane of the sample surface ply. When the panel was oriented horizontally, the fiber direction in the surface ply was parallel to the projection. When oriented vertically, the surface ply direction was perpendicular to the projection.

Cumulative sample mass loss was plotted versus the cumulative mass of the erodent particles striking the sample. Although there are usually some initial transients, the data typically fall on a straight line. The slope of this line is the steady-state wear rate ΔW in dimensionless units of mass per mass. In addition to the steady-state experiments, samples were polished and exposed to the erodent for a very short time. Single-impact sites could then be examined by this method.

It is estimated that the average mass-loss measurements were accurate to ±5%. When metal samples have been eroded on this apparatus, the steady-state erosion rates have been reproducible over long times (a few years) within 10%. It is anticipated that this figure may be slightly higher (less than 20%) in the ceramic composites due to the irregular surfaces which develop during erosion.

The erodent particles used for these experiments were angularly-shaped SiC* particles with average diameters of 42 μm (280 grit), 63 μm (240 grit), 143 μm (100 grit), and 390 μm (54 grit). Impact angles used were 30° and 90°. Impact velocities were 30 m/sec, 50 m/sec and 80 m/sec.

C. Scanning Electron Microscopy

Both the single-impact and steady-state eroded surfaces were examined by scanning electron microscopy (SEM)§.

Results & Discussion

A. Steady-State Erosion Measurements

The steady-state wear rates for an erodent velocity of 50 m/sec are given in Table I. Table II gives the erosion data for 54 grit (390 μm) erodent particles at various velocities. For angles less than 90° panels were tested in both horizontal and vertical orientations. At a 90° angle, there is no distinction between horizontal and vertical. (The projection is a point.) These orientation conventions do not apply to the composites made with the woven fabric, as fibers in each ply are oriented in two-dimensional weave.

Figure 1 and Figure 2 show the steady-state erosion rates for the various composites when the erodents strike the surfaces at 30° and 90° angles, respectively. Notice that there is very little difference between the data for the weave and the 0/90 unidirectional layup. Thus, varying the fiber orientation parallel to the composite surface does not appear to affect erosion rate. Surprisingly, there also is very little difference between the data

* Crystolon, Norton Co., Worcester, MA.

§ JEOL JXA-840A SEM.

for the oxidized and non-oxidized composites. Tensile and flexural properties for composites treated in these two ways differ significantly. However, there is little effect upon erosion properties.

On first discusion we can assume that the Blackglas™ matrix has mechanical properties similar to fused silica (SiO_2). To that end fused silica glass test panels were used as a comparable control. In all cases - but particularly for larger eroding particles - the Blackglas™ composites erode more rapidly than the SiO_2. This is shown for erosion at 30° and 90° in Figure 3 and Figure 4, respectively. If we assume that a pure Blackglas™ matrix material would have erosion properties similar to those of silica glass, the introduction of fibers results in an increase in erosion rate. In previous work, we also saw a similar increase when fibers were introduced into an epoxy matrix[1].

It should be noted that the Blackglas™ matrix in the composite differs from fused silica in one major respect; it is not fully dense or crack free. This condition is a result of the multiple infiltration/pyrolysis densification method. It is a general characteristic of all the polymer precursor fabrication routes. Thus, it is possible that the perceived increase in erosion rate is attributable to the porosity of the matrix.

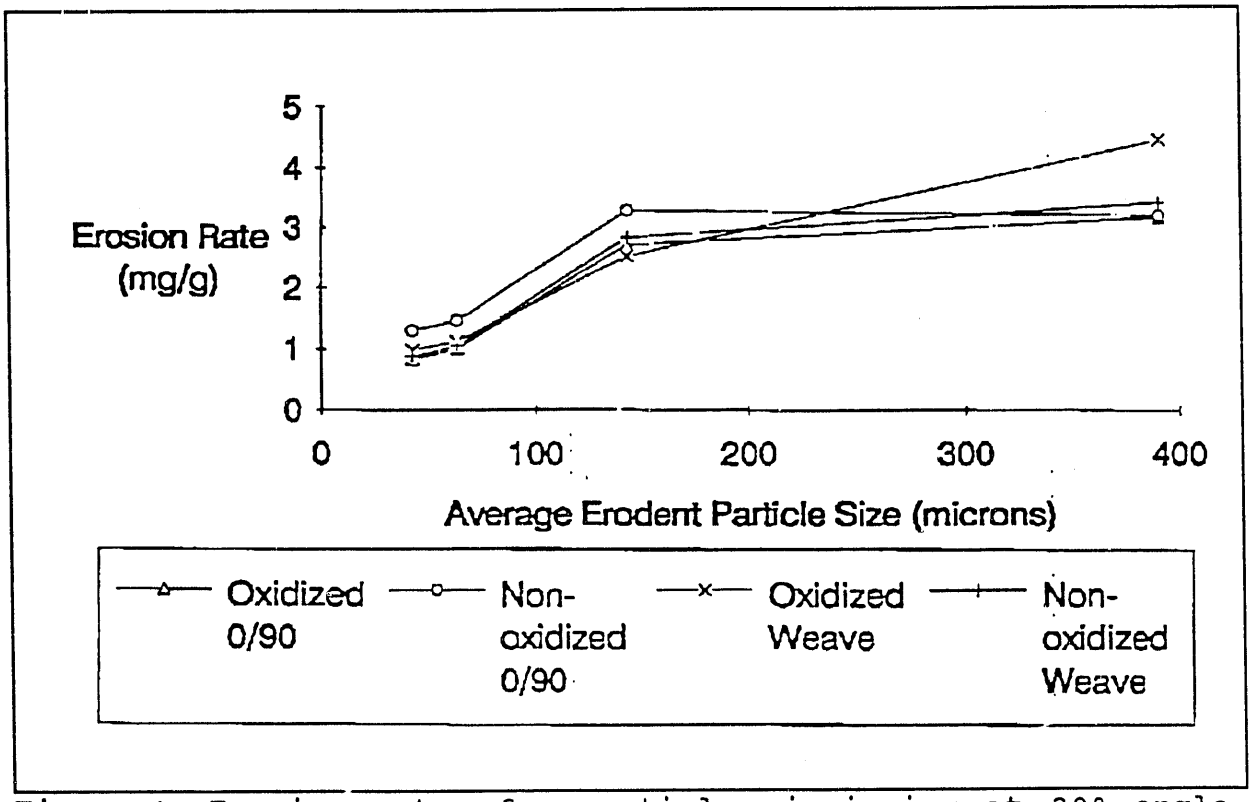

Figure 1 Erosion rates for particles impinging at 30° angle. (Points are connected for clarity only.)

Table I Erosion Data: Particle-Size Dependence
(mg wt. loss per g of erodent)

	α(°)	orientation	Sample #	54 Grit 390 μm	100 Grit 143 μm	240 Grit 63 μm	280 Grit 42 μm
C-Coated-Nicalon Black Glass Oxidized Composite	90	Horizontal	A4		4.982	1.865	1.278
	30	Horizontal	A5		2.716	1.024	0.838
	30	Vertical	A6			1.455	
	90	Horizontal	A1	8.668			
	30	Horizontal	A2	3.169			
	30	Vertical	A3	3.767			
C-Coated-Nicalon Black Glass Non-oxidized Composite	90	Horizontal	B4		5.431	2.427	1.865
	30	Horizontal	B5		3.278	1.476	1.305
	30	Vertical	B6			2.535	
	90	Horizontal	B1	7.163			
	30	Horizontal	B2	3.191			
	30	Vertical	B3	3.418			
C-Coated-Nicalon Black Glass Oxidized Weave Composite	90	Horizontal	D1	7.275	4.052		1.377
	30	Horizontal	D2	4.467	2.526		1.000
	90	Horizontal	D3			1.810	
	30	Horizontal	D4			1.140	
C-Coated-Nicalon Black Glass Non-oxidized Weave Composite	90	Horizontal	E3	7.390	4.831		1.618
	30	Horizontal	E2	3.410	2.838		8.838
	90	Horizontal	E1			1.755	
	30	Horizontal	E4			1.064	
Fused Silica	90		C3			1.329	
	90		C4		2.621		1.159
	30		C5		1.176		0.670
	90		C2	4.705			
	30		C1,C3	2.147			

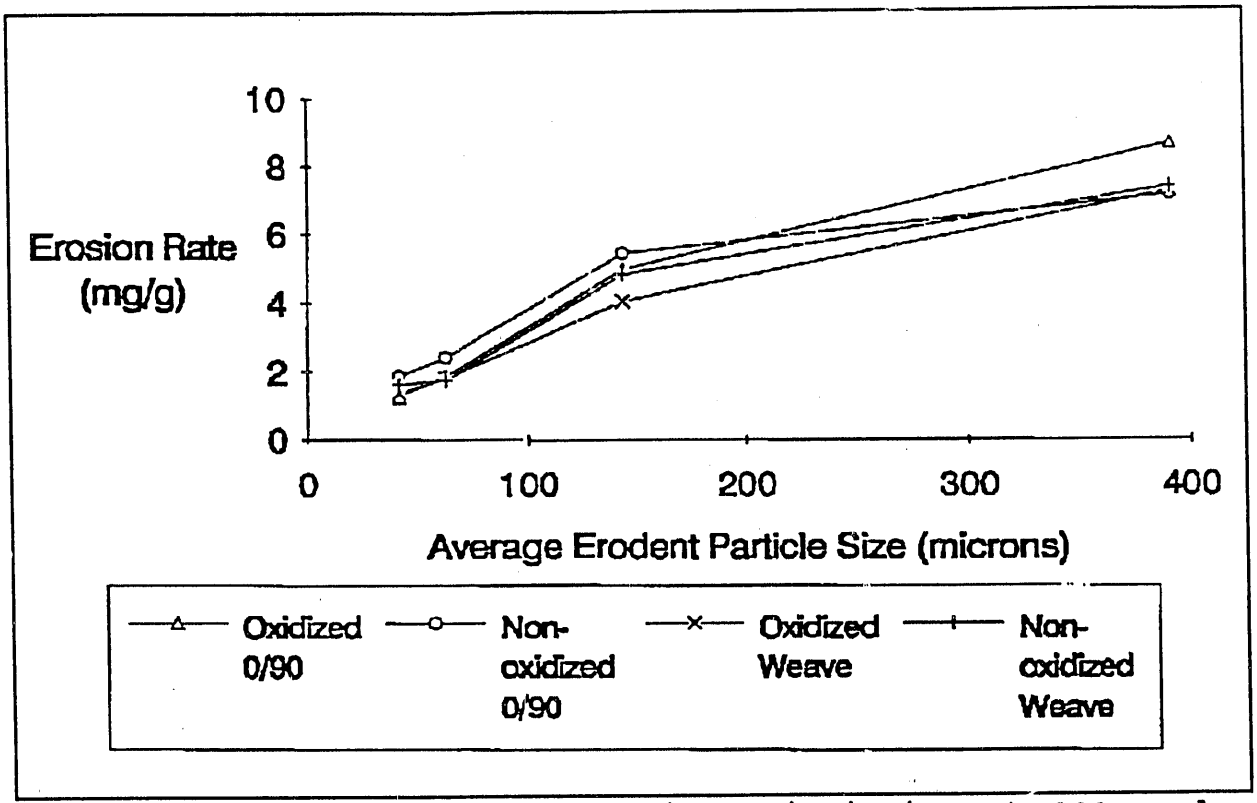

Figure 2 Erosion rates for particles impinging at 90° angle. (Points are connected for clarity only.)

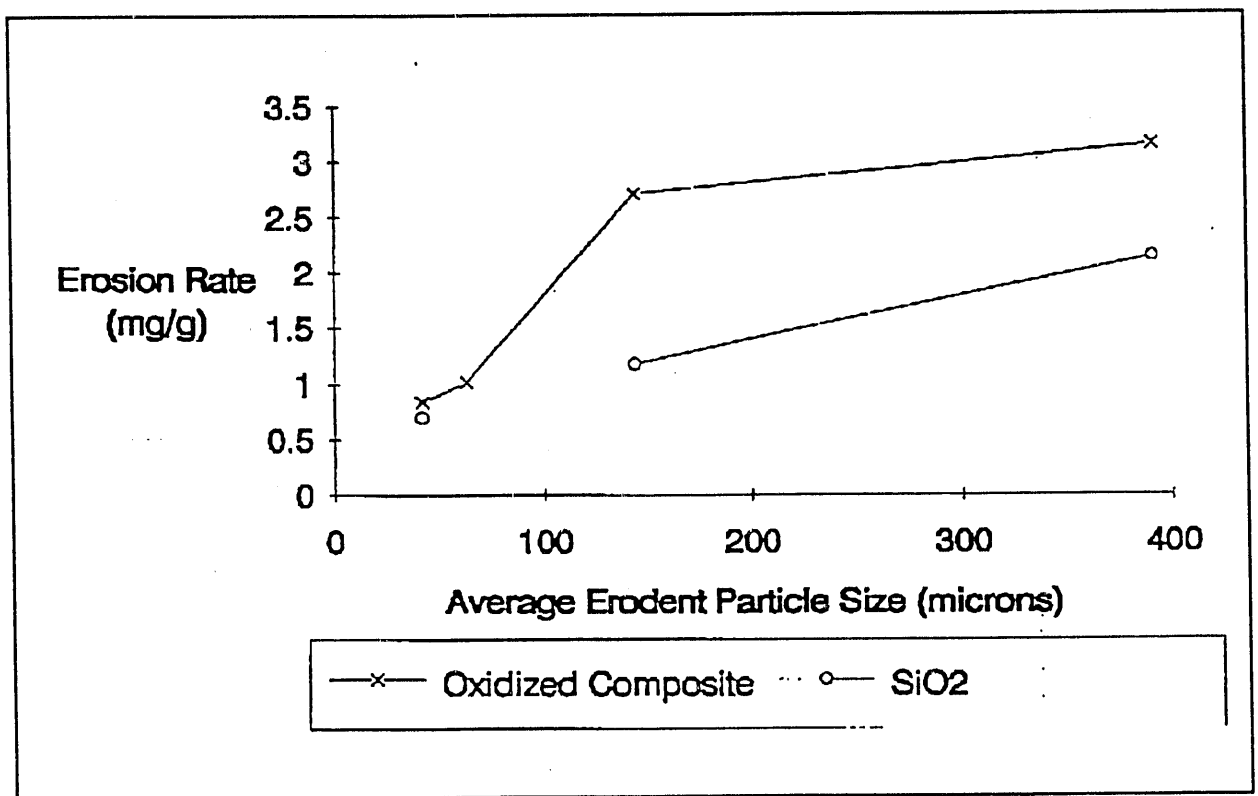

Figure 3 Comparison of erosion rates in Blackglas™ composites and fused SiO_2 at 30° angle. (Points are connected for clarity only.)

Table II Erosion Data: Velocity Dependence
(mg wt. loss per g of erodent)

	α(°)	orientation	Sample #	30 m/sec	50 m/sec	80 m/sec
C-Coated-Nicalon Black Glass Oxidized Composite	90	Horizontal	A1	2.71	8.67	42.87
	30	Horizontal	A2	1.93	3.17	14.85
	30	Vertical	A3	1.65	3.77	15.68
C-Coated-Nicalon Black Glass Non-oxidized Composite	90	Horizontal	B1	2.6	7.16	23.31
	30	Horizontal	B2	2.19	3.19	11.68
	30	Vertical	B3	2.16	3.42	12.09
Fused Silica	90		C2	1.41	4.71	20.59
	30		C1,C3	0.59	2.15	9.26

Figure 5 shows the velocity dependencies of the erosion data for 54 grit (390 μm) erodent particles for impacts at 90°. The slopes appear to be on the order of 2 to 3. Drawing any quantitative conclusions is difficult, however, since the velocity varies by less than one decade.

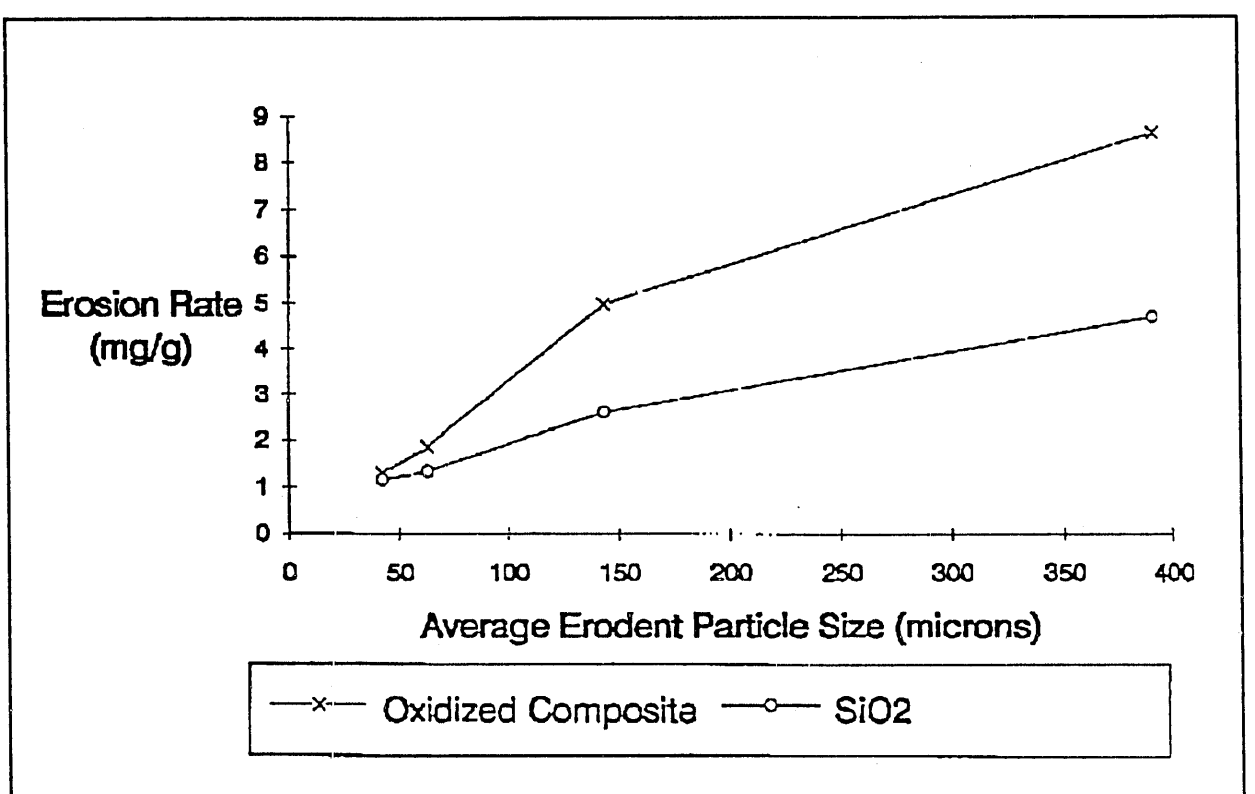

Figure 4 Comparison of erosion rates in Blackglas™ composites and fused SiO_2 at 90° angle. (Points are connected for clarity only.)

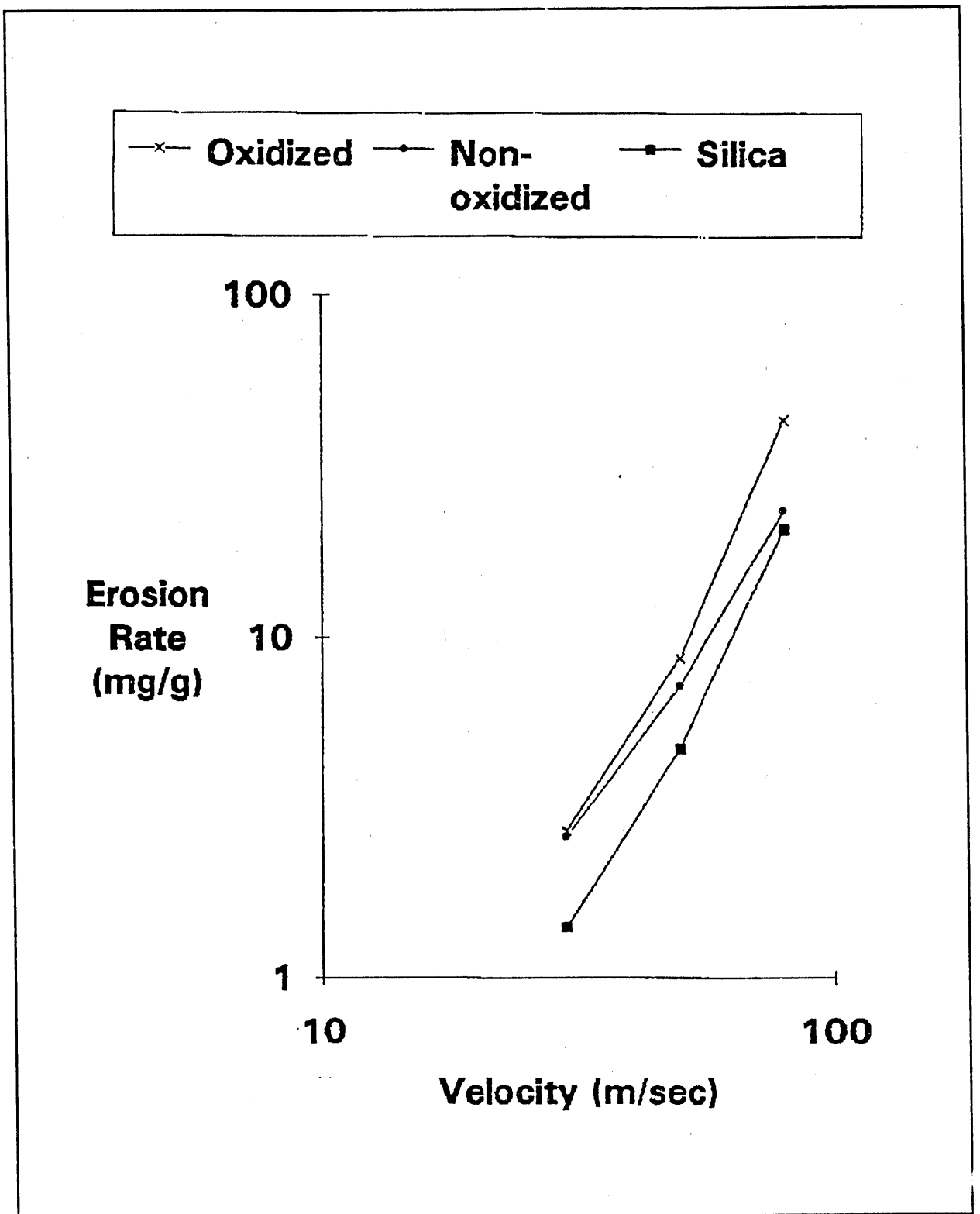

Figure 5 Velocity dependence of the erosion rate in Blackglas™ composites.

B.Scanning Electron Microscopy

Photomicrographs are displayed in Appendix A.

The steady-state erosion surfaces were examined by SEM. An example is given in Figure A.1, where the surface of a non-oxidized sample made with a woven fabric eroded by 54-grit particles traveling at 50 m/sec at a 90° angle is displayed. Such views are difficult to interpret due to the overlapping effects of multiple impacts.

Somewhat more revealing are single-particle impacts on polished surfaces. Figure A.2 shows this type of impact in an oxidized sample made with unidirectional laminate eroded by a 54-grit particle traveling at 50 m/sec at a 90° angle. In contrast, Figure A.3 shows the damage under similar conditions on a silica surface. This last micrograph is typical for monolithic brittle materials. While it is not completely symmetric, the damage does appear to progress radially, In contrast, the fibers in the composite appear to guide the cracks.

The SEM photographs of the single-particle impacts are similar to single-particle impacts that we have seen in previous work on carbon-fiber-reinforced-BMI-epoxy composites[3]. In that work the fibers also appeared to guide the lateral cracks. The equivalent micrographs of the unreinforced polymer[4] resembled those of the silica in the current study.

C. Erosion Theory

(A more detailed discussion of erosion theories with references can be found in the recent review published by Routbort and Scattergood[5].)

Evans, et al[6]. performed finite difference calculations to model the impact of a solid particle upon a brittle material. This model showed that upon impact a plastic wave front propagates into the brittle material beneath the particle. The stress in this plastic zone is compressive. Directly ahead of the plastic zone is an elastic zone in which the stresses are tensile. According to the model the tensile stresses are largest when the particle rebounds. The maximum tension occurs in the elastic region close to the elastic-plastic interface; it is tangential rather than radial stress. It is probably during this unloading period that lateral cracks form parallel to the surface. In addition there are radial cracks which curve upward and intersect the surface. The amount of material removed is governed by the depth of the lateral cracks and the diameter of the radial cracks.

For a quasi-static load situation (e.g., indentation), Evans and Wilshaw[7] calculated the relationship between the contact stress p and the radial crack extension C_r. Evans, et al[6]. then assume that the dynamic contact pressure and radius follow the same functional relationship during the loading and unloading process. From this they assert that the crack length will be determined by the time at which a product of the contact pressure (with which the stress amplitude scales) and contact radius (with which the size of the

stress field scales) attains a maximum. They then make two extreme estimates of this critical time. First, they assume that it coincides with the return of the longitudinal wave in the erodent particle to the interface. This is plausible, as one would expect the pressure to drop off rapidly after this point. Alternately, they assume that it occurs when the particle achieves full penetration. From these estimates the contact pressure and radius can be calculated and from these C_r is determined. Both calculations result in similar functional forms for the crack length.

While Evans, et al[6]. performed a detailed stress analysis, Wiederhorn and Lawn[8] made a much simpler analysis based upon energy balance. They assumed that all of the kinetic energy of the erodent particle is converted into plastic flow of the target material.

Both theories predict a steady-state erosion rate in the form:

$$\Delta W \propto V^n D^{2/3} \rho^p (K_{Ic})^{-4/3} H^q \qquad (1)$$

where V, D, and ρ are the velocity, diameter, and density, respectively, of the impinging particles, and K_{Ic} and H are the toughness and hardness, respectively, of the target material. ΔW is essentially dimensionless, being measured in terms of mass of target material eroded per mass of erodent material. The velocity exponent n depends upon the geometry of the erodent particles, typically varying between 2 and 3.2 (although it can be as low as 0.67 for a cylinder). The density exponent p is 1.2 to 1.3, while the hardness exponent q is -0.25 for the micromechanics model and 0.11 for the energy-balance model. This equation holds for normal incidence; for an angle α other than 90°, the velocity should be replaced by $V\sin\alpha$.

D. Angular Dependence

From Equation (1) one would expect the ratio of the erosion rate at angle α to that at angle 90° to be:

$$\Delta W(\alpha)/\Delta W(90°) = (\sin\alpha)^n \qquad (2)$$

Since n is typically on the order of 2, for α=30° we expect the ratio to be about 0.25. The ratios computed from the data in Table I are given below in Table III.

The ratios are much higher than would be expected from Equations (1) and (2). Higher erosion rates than predicted at low angles are not uncommon; we saw such behavior in the erosion of epoxy polymers[1,3]. This may indicate failure of the model or the operation of another fracture mode.

Table III $\Delta W(30°)/\Delta W(90°)$

Avg. Particle Size (microns)	390	143	63	42
Oxidized Composite	0.37	0.55	0.55	0.66
Non-oxidized Composite	0.45	0.60	0.61	0.70
Oxidized Weave Composite	0.61	0.62	0.63	0.73
Non-oxidized Weave Composite	0.46	0.59	0.61	0.55
Fused Silica	0.46	0.45		0.60

E. Micromechanics of Composites

The ratio of erosion rate of the matrix to that of the composite is less than 1. However, it never falls below 1/3 and is often greater than 1/2 - particularly for small erodent size.

The models discussed in the last section assume that the brittle material being eroded has isotropic mechanical properties. This is obviously not true for composites. In the Blackglas™ composites the Nicalon™ fibers have a higher stiffness, strength, and hardness than the matrix material. The acoustic impedance is much lower. The elastic strains and any deformation in the fibers will be minimal compared to those in the matrix, even though the matrix occupies approximately half the volume that the fibers do.

Since the lateral cracks propagate parallel to the fibers, the situation is similar to transverse tensile fracture of the composite. The stress in the matrix is not uniformly distributed; there is a stress concentration in the matrix at the fiber-matrix interface[9]. The result is that the transverse tensile strength of a brittle-matrix composite is less than the matrix tensile strength. In addition, once the matrix is degraded, fibers can be removed easily by erosion. Thus, it is quite plausible that the composite (with fibers oriented parallel to the surface) is much more susceptible to erosion than the unreinforced matrix.

Of course, the erosion situation is somewhat more complicated than transverse fracture. The lateral cracks do bend up eventually and break through to the surface. Several theoretical models have been proposed to predict unidirectionally reinforced polymer composite strength[10] as a function of angle between the fibers and the impact-load direction. The strength is a minimum for transverse orientation and a maximum for longitudinal orientation. Thus, the

situation for erosion is probably not as harsh as that for transverse fracture.

Since much of erosion involves transverse fracture due to the parallel fiber orientation, one solution to the problem may be to modify the fiber weave. For example, a three-dimensional weave would provide fibers perpendicular as well as parallel to the surface. It would be much more difficult for cracks to avoid fibers in this case. A suggestion for future work is to model the indent stresses in a composite by a finite-element or finite-difference technique. This might then enable one to engineer an appropriate weave pattern. (One word of caution should be made. None of the composite theories account for fracture toughness of the materials. Thus, one could calculate stress distributions but may not be able to calculate actual strengths.)

Conclusions and Recommendations

The primary observation from this work is that the inclusion of fibers in a brittle microcracked ceramic matrix produces a material which is less erosion-resistant than the matrix. Specifically, Blackglas™ matrix composites are more susceptible to erosion than fused silica. In the experiments in this study the composites typically eroded two to three times faster than silica (for 90° attack angle). This should be recognized in any potential application which may involve erosive conditions.

It is possible that the increased erosion rate is attributable to the porosity and microcracking in the matrix. However, previous experience with brittle-polymer-matrix composites and theoretical considerations imply that any ceramic matrix is likely to have increased susceptibility to erosion when fiber reinforcements are added.

References

1. K. R. Karasek, K. C. Goretta, D. A. Helberg, and J. L. Routbort, "Erosion in BMI polymers and BMI-polymer composites," submitted to J. Materials Science Letters.

2. T. H. Kosel, R. O. Scattergood, and A. P. Turner, "An electron microscopy study of erosive wear"; pp. 192-204 in Wear of Materials. Edited by K. C. Ludema, W. A. Glaeser, and S. K. Rhee. American Society of Mechanical Engineers, New York, 1979.

3. P. J. Mathias, W. Wu, K. C. Goretta, J. L. Routbort, D. P. Groppi, and K. R. Karasek, "Solid particle erosion of a graphite-fiber-reinforced bismaleimide polymer composite," Wear **135** 161-9 (1989).

4. A. Brandstädter, K. C. Goretta, J. L. Routbort, D. P. Groppi, and K. R. Karasek, "Solid-particle erosion of bismaleimide polymers," Wear **147** 144-64 (1991).

5. J. L. Routbort and R. O. Scattergood, "Solid-particle erosion of ceramics and ceramic composites," in Erosion of Ceramic Materials, edited by J. E. Ritter. Trans Tech Publications, Ltd. (1991).

6. A. G. Evans, M. E. Gulden, and M. Rosenblatt, "Impact damage in brittle materials in the elastic-plastic regime," Proc. Roy. Soc. London **A361** [1706] 343-65 (1978).

7. A. G. Evans and T. R. Wilshaw, Acta Metall. **24** 239-56 (1976).

8. S. M. Wiederhorn and B. R. Lawn, "Strength degradation of glass impacted with sharp particles: I," J. Am. Ceram. Soc. **62** [1-2] 66-70 (1979).

9. S. W. Tsai and H. T. Hahn, *Introduction to Composite Materials*; pp. 416-9. Technomic Publishing Company, Inc., Lancaster, PA, 1980.

10. B. D. Agarwal and L. J. Broutman, *Analysis and Performance of Fiber Composites*; pp. 132-9. John Wiley & Sons, New York, 1980.

Appendix A

SEM Micrographs

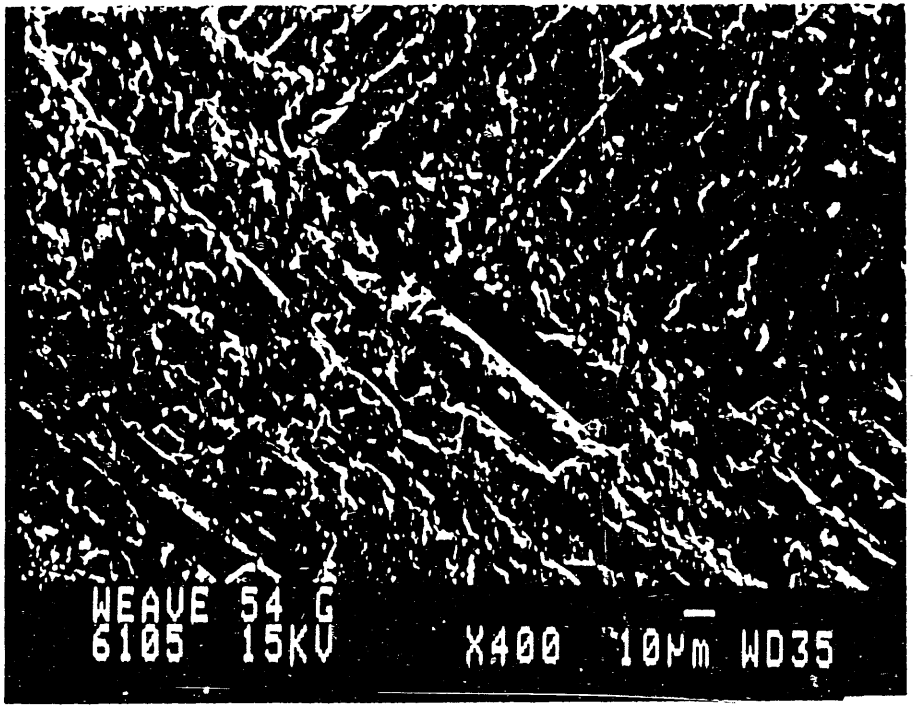

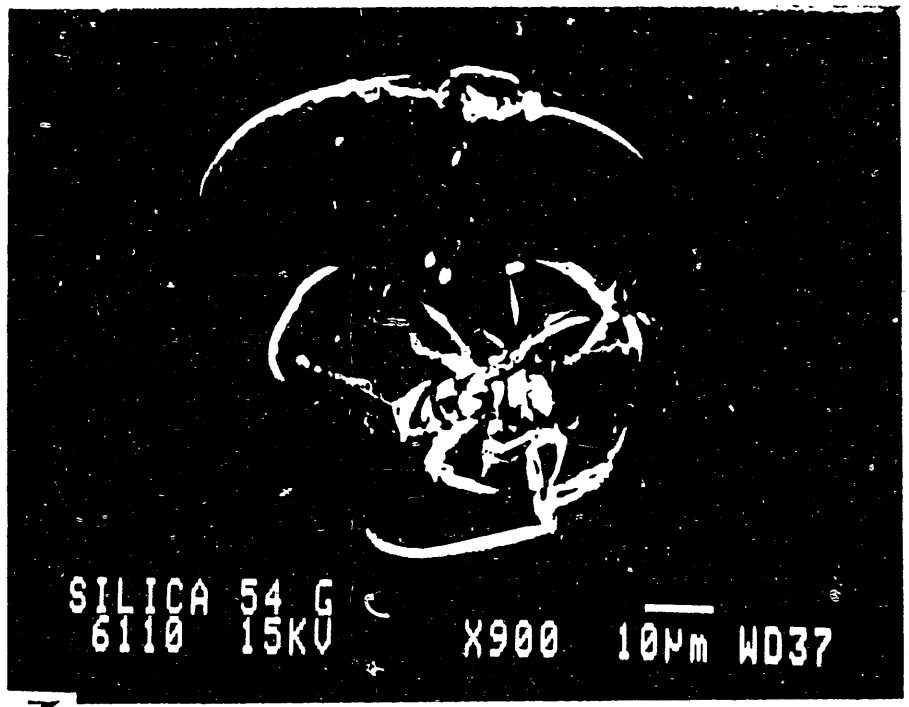

A.1 A.3

A.2

Figure A.1: Steady-state erosion of non-oxidized woven-fabric composite by 390 µm particles traveling at 50 m/sec impinging at 90°.

Figure A.2: Single-particle impact on an oxidized unidirectional-laminate composite by a 390 µm particle traveling at 50 m/sec impinging at 90°.

Figure A.3: Damage under same conditions as A.2 but on a silica surface.

END

DATE FILMED

3/5/92